International Journal of Mechanical and Production Engineering Research and Development (IJMPERD)
ISSN(P): 2249-6890; ISSN(E): 2249-8001
Vol. 8, Issue 6, Dec 2018, 643-660

AN EXPERIMENTAL INVESTIGATION OF HEAT TRANSFER AND FRICTION FACTOR IN SOLAR AIR HEATER DUCT USING DOUBLE ARC REVERSE SHAPED RIB ROUGHNESS ON ABSORBER PLATE

YOGESH AGRAWAL & J. L. BHAGORIA

Department of Mechanical Engineering, Maulana Azad National Institute of Technology, Bhopal, Madhya Pradesh, India

ABSTRACT

A solar air heater is a thermal system that uses artificial roughness in the form of repeated ribs on the absorbent plate to improve the rate of heat transfer. An experimental study was conducted to investigate the thermo hydraulic performance using Double arc reverse shaped ribs in the air absorption plate that passes through the rectangular duct, the rough wall is heated while the other three walls are insulated. The roughness of the wall have a pitch (p) of 10 mm, the relative roughness pitch (p/e) = 8.33, the height of the rib (e) is 1.2 mm, the height of the relative roughness (e /Dh) of 0.027 and the flow of air corresponds to the Re between 3000 and 14000. The arc angle of the roughness geometry varies between 30^0 and 75^0. The results of the heat transfer were compared with those of the smooth ducts under similar flow conditions and thermal limits to determine the thermal efficiency of the solar air heater. The convection heat transfer coefficient and the Nu increase with increasing Re for a unique Double arc reverse shaped rib roughness. The increase in Nu is 1.26 to 2.478 & the f is 1.40 to 1.74 times compared to the smooth plate respectively. Roughness also increases the value of the friction factor, but the increase in its value is small compared to the increase in the heat transfer coefficient. The maximum improvement in the Nu is 2.478 for the pitch of 10 mm, the arc angle of 75^0 for the Re 14,000 in comparison with the smooth plate. Thermo hydraulic yields show a first increasing variation, and then decrease with respect to the increase in the Re. The maximum improvement in thermo hydraulic performance is observed with the Re 7000, pitch of 10 mm and the arc angle of 75^0 with respect to the smooth plate, after which it begins to decrease with the increase in the Re.

KEYWORDS: Double arc Reverses Shaped Roughness, Pressure Drop, Solar Air Heater & Thermo Hydraulic Performance

Received: Oct 07, 2018; **Accepted:** Oct 27, 2018; **Published:** Dec 06, 2018; **Paper Id.:** IJMPERDDEC201867

Original Article

NOMENCLATURE

A_c	Surface area of absorber plate, (m^2)	**Nu**	Nusselt number
A_o	Area of orifice meter, (m^2)	**p**	Pitch (m)
C_d	Coefficient of discharge	**p/e**	Relative roughness pitch
C_p	Specific heat of air (KJ/kg K)	$(\Delta P)_o$	Pressure drop of orifice plate (Pa)
D_h	Hydraulic diameter of air passage	$(\Delta P)_d$	Pressure drop of duct (Pa)
e	Rib height, (mm)	Q_a	Useful heat gain (W)
e/D_h	Relative roughness height	**Re**	Reynolds number

f	Friction factor	$\mathbf{T_a}$	Atmospheric air temperature (^oC)
H	Height of air channel (m)	$\mathbf{T_{fav}}$	Average fluid flow temperature (^oC)
h	Heat transfer convective coeff ($W/m^2 K$)	$\mathbf{T_i}$	Inlet fluid temperature (^oC)
Δh	Difference of height on Manometer fluid (mm)	$\mathbf{T_o}$	Outlet fluid temperature (^oC)
I	Heat Flux (W/m^2)	$\mathbf{T_p}$	Average plate temperature (^oC)
k	Thermal conductivity of air, (W/m-K)	**V**	Velocity of air, m/s
L	Length of test section in duct (m)	**W**	Width of air duct, m
m	Mass flow rate of air (kg/s)	**W/H**	Width to height of duct ratio

Greek Symbols

α	Arc angle (^{0})
β	Ratio of orifice diameter to pipe diameter
η	Thermal Efficiency
ρ	Density of air (kg/m^3)
$\mathbf{\rho_m}$	Density of Manometric fluid (kg/m^3)
ν	Kinematic viscosity of air (m^2/s)

Subscripts

a	Ambient
f	Fluid Flow
i	Inlet
o	Outlet
s	Smooth channel

1. INTRODUCTION

Due to population growth and industrial development, the demand for energy is increasing day by day. The availability of solar energy and its ecological nature are two characteristics that make solar energy the most favourable among alternative energy sources. Solar energy is the light and radiant heat of the sun that impacts the Earth's atmosphere and climate and is compatible with life. It is considered a great source of energy that is freely available without leaving any effect on the environment. For solar energy as an access point for renewable energies, look at solar or photovoltaic energy upwards. Sun-based advances are largely delineated as passive solar energy or active solar energy, depending on the method captured, changed and disseminated by solar energy. Most strategies based on active sunlight integrate the use of panels with electrical phenomena and authorizations of solar heat to equip energy. Inactive solar procedures incorporate the composition of a building to the sun, selecting materials with ideal diffusion or heat dispersion properties, and describing the spaces where air generally circulates. Solar energy is used to heat with the help of a solar collector. Solar air heaters, for its simplicity and low cost. As the air passes over the absorbent plate, it produces a laminar and turbulent surface on the surface, due to the formation of a lower laminar layer that reduces the rate of heat transfer because it acts as a resistance to flow thermal. To overcome this phenomenon and improve heat transfer, we create an artificial roughness on the bottom of the absorbent plate. The artificial roughness breaks the laminar sub layer and creates turbulence that causes an increase in the rate of heat transfer. In the research area of solar air heater, many researchers have proposed various artificial roughness geometries for the enhancement of heat transfer rate. In the literature given in this

paper, various designs suggested by researchers are discussed. [1-3]

Prasad and Mullick [4] experimentally investigated the effect of a small diameter wire attached to the underside of the absorbent plate as an artificial roughness. Prasad et al. [5] studied the fundamental of the roughened absorber plate by attaching small diameter wires in the transverse position. They take rib roughness pitch 10 – 20, relative roughness height, e/D_h 0.02 – 0.033. Han and Park [6] carried out experimental studies using inclined ribs in elongated form factor tubes that show a considerable increase in the improvement of heat transfer. Experimental research by Gupta et al. [7] reported that the Stanton number initially increased to a Reynolds number of 12,000, then decreased to further increase the Reynolds number by providing a transverse wire such as artificial roughness in the absorbent plate in the solar air heater. Saini and Saini [8] applied the artificial roughness in the form of circular wires and expanded metal, respectively, in the form of artificial roughness on the inner surface of the absorbent plate of the solar air heaters. Karwa et al.[9] proposed the use of integrative chamfered ribs to improve the Stanton number and the friction factor up to approximately twice and three times, respectively, for 15^0 chamfer angles. Verma et al. [10] performed an outdoor experiment on circular ribs taking the Reynolds number, Re 5000 - 20,000, the relative pitch, p was 10 to 40 and the relative roughness height p/e from 0.01 to 0.038. Karwa et al. [11] conducted an experimental study using chamfered ribs. The presence of chamfered ribs leads to an increase of 2 times the number of Stanton and 3 times the friction factor. The highest happened for the 15º chamfer. With the increase in the aspect ratio, W / H from 4.65 to 7.75, the roughness function decreased. Momin et al. [12] conducted an experimental study using the V-shaped rib as a roughness parameter. Reynolds number value, Re was 2500-18000 with a relative roughness pitch, p/e of 20 mm. Bhagoria [13] has been Experimentally studied with wedge shaped transverse integral ribs, the effect of relative roughness pitch (p/e) relative roughness height (e/D_h) and wedge angle (ϕ) on the heat transfer coefficient and the friction factor in solar air heater rectangular duct. Sahu et al. [14] experimentally investigated the effect of 90^0 broken transverse ribs for improving hydraulic performance of solar air heater by taking roughness height, e as 1.5 mm, aspect ratio of 8 and range of Reynolds number was between 3000-12000. Karmare et al.[15] conducted an experimental study by taking grid of metal ribs of circular cross section as roughness elements. Relative roughness height, e/D_h of 0.035 – 0.044, having relative roughness pitch, p/e of 12.5 – 36 and range of Reynolds number, Re was 4000 – 17000. Aharwal et al. [16] experimentally investigated the effect of width and position of gap in inclined split ribs having square cross sections on heat transfer and friction characteristics of rectangular solar air heater duct. Kumar et al. [17] experimentally studied heat transfer characteristic by taking discrete W – shaped rib as roughness element. Range of Reynolds number, Re was between 3000 – 15000 having relative roughness height, e/D_h 0.0168 – 0.0337 and angle of attack, α of 30º - 75º. Hans et al. [18] reported that the inclination and orientations of ribs with the flow direction also affects the heat transfer and friction through the roughened duct. The use of multiple V-shape ribs results the formation of secondary flow and hence the more turbulence; leading to high heat transfer. Sethi et al. [19] examined dimple shaped roughness. The range of parameters was investigated and covered by duct aspect ratio (W/H) 11, relative angle of attack $47\text{-}75^{0,}$ Reynolds number (Re) from 3600-18,000, relative roughness height (e/D_h) as 0.021-0.036. Yadav et al. [20]. Numerically investigated of turbulent flows through a solar air heater roughened with semicircular sectioned transverse rib roughness. The thermo hydraulic performance parameter is found to be the maximum of the relative roughness height of 0.042. Singh et al. [21] Conducted experiment by using multiple arc shaped ribs as roughness on the absorber plate. He used relative roughness pitch, p/e of 4-16, relative roughness height, e/D_h of 0.018-0.045 and Reynolds number, Re varied between 2200-22000. Lanjewar et al. [22] experimentally investigated for the friction characteristics and heat transfer coefficient with different orientation of double arc rib roughness to enhance the thermo-hydraulic performance of the solar

air heater. Maithani et al. [23] performed experimental study for finding the effect of symmetrical multiple gaps in V – shaped ribs. Angle of attack, α was 30º - 75º, relative rib pitch varied from 6 – 12. Hans et al. [24] experimentally studied correlation on heat transfer and friction factor for solar air heater by taking a broken arc rib as a roughness parameter on the absorber plate. Mohit kumar et.al. [25] Experimentally examined C type multiple shaped roughness. Correlations were developed for Nusselt number, friction factor, Stanton number and Thermo hydraulic performance parameter to increase the usefulness of the result.

2. EXPEIMENTAL SET UP

To determine the performance of the rectangular duct by using the artificial roughness of double arc reverse shape continuous rib, we obtained data like heat transfer coefficient, friction factor and thermal efficiency by using an experimental set up. Using experimental data, we compared the performance of a rectangular duct with a smooth plate and a continuous double-arc reverse shaped with different arc angles. In general, we try to increase the coefficient of heat transfer and the thermo hydraulic performance of rectangular ducts with a higher thermal efficiency.

An experimental facility was designed and manufactured to study the effect of double-arc reverse ribs on the characteristics of heat transfer and fluid flow in a rectangular duct for a range of parameters chosen according to the practical considerations of the system and the operating conditions. The experimental test section comprises a wooden channel comprising five sections, namely a smooth inlet section, a roughened inlet section, a test section, an outlet section or a mixing section. A G.I. sheet of 20 SWG (standard wire gauge) of 0.3 m^2 size has been used as an absorber plate and lower surface of the plate has been provided with artificial roughness in form of Reverse shaped copper wires. An electric heater of dimensions identical to that of absorber plate has been used to provide uniform heat flux to the absorber plate up to maximum of 1500W/m^2. Power supply to heater has been provided through variable transformer. Transformer enables heat flux applied to the absorber plate to be varied as desired. Schematic diagram of the experimental set up and view of plate with the roughness geometry of Double arc reverse shaped ribs are shown in Figure 1. Double arc reverse-shaped roughness elements were fixed below the absorber plate and fast drying epoxy has been applied for gluing roughness elements. Values of system and operating parameters of this investigation are listed in Table. Relative roughness pitch (p/e) value has been selected as 8.33, based on optimum value of this parameter reported in literature. The dimensions used for te flow section of experimental set up are shown below in Fig.1. In the cross section view with rough plate.

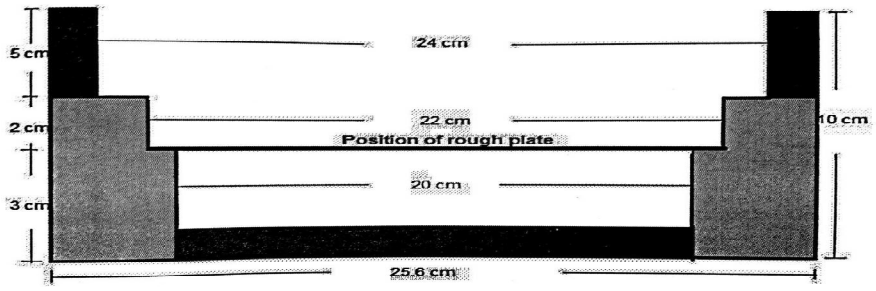

Figure 1: Cross Section View of Flow Section

The duct is made of wooden panels of size 25 mm thickness having dimension of the inner cross section is 2042 mm * 200 mm * 20 mm as shown above in the figure. The test section is 1500 mm long and entry and exit section or mixing section is 192 mm and 350 mm long respectively. In terms of equivalent diameter of air passage (D_h):

- Entry section= 7.2 D_h
- Test section= 33.75 D_h
- Exit section or mixing section= 12 D_h

The entry section is from where the air enters with atmospheric temperature, test section where the experimental test performs on the rough plate having Double arc reverse shape roughness ribs and exit section to take output temperature. Entry section is provided to measure air inlet temperature and so that flow can be converted into fully developed flow. The position of rough plate on the duct is shown in Fig.1. The pressure drop across the orifice is measured using U-tube Manometer and mass flow rate is calculated. The air flow rate is controlled by using a flow control valve provided with the pipe. As per the recommendation of Preobrazensky the diameter of orifice plate is designed for the flow measurement inside the pipe is taken as 53 mm, the orifice plate is arranged between the flanges to align it concentric with the pipe as shown in Figure 2 of experimental setup. The calibrated thermocouple wires of copper-constantan is used to measure the temperature difference of air and heated plate in the form of electromagnetic force generated by sea back effect. Being indoor type experimental setup, the artificial solar radiations are generated on the absorber plate, an electric heater of size 1650 mm * 216 mm was fabricated by arranging heating wires in series and parallel loops on 5 mm asbestos sheet. A mica sheet of 1 mm thickness is provided in between the absorbing plate and heater which acts as an insulator. Heat flux may be varied from 0 to 1500 W/m^2 by using variac. The entire duct is covered with 12 mm thick plywood to insulate the whole assembly.

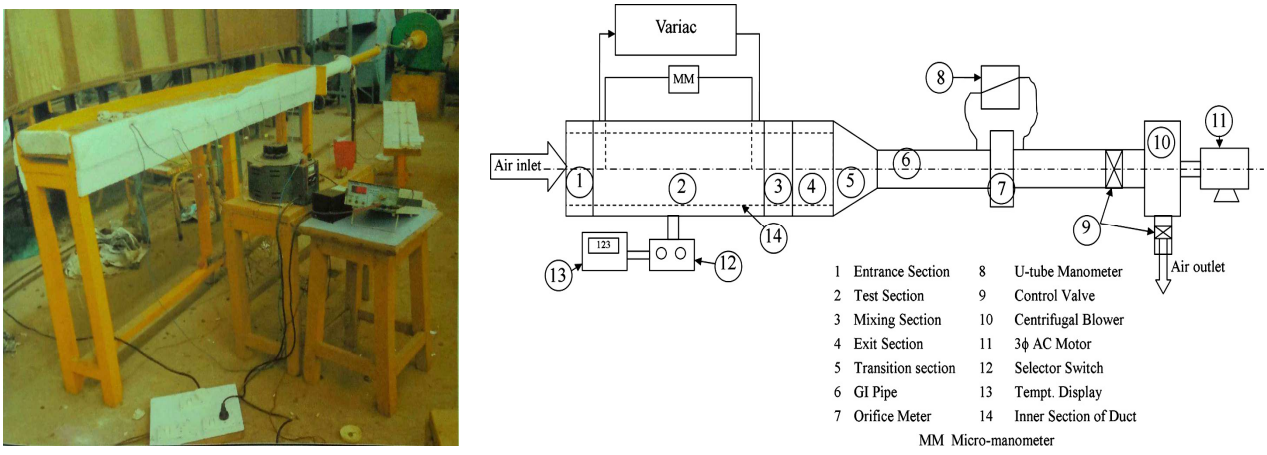

Figure 2: Schematic Diagram of Experimental Setup

The experimental Data is collected by using different instruments for different angle of attack of the roughness geometry of the absorbing plate shown in Figure 3. The air flow rate changes by using control valve and the data obtained of the roughened plate is compared with the smooth plate. This experimental data has been used to determine the heat transfer coefficient, friction factor, Nusselt number and thermal efficiency.

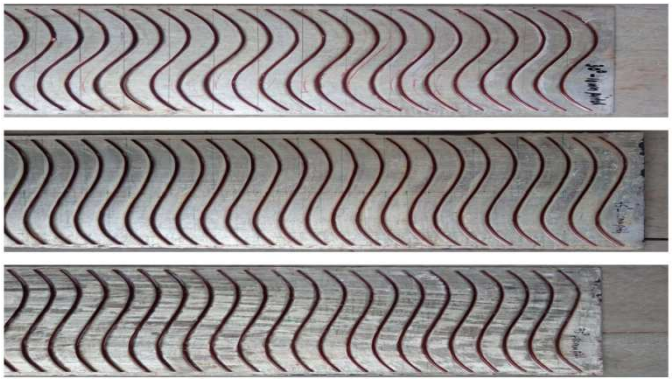

Figure 3: Artificial Roughness (Double arc Reverse Shaped) of Pitch 10mm and at Different Angles

3. EXPERIMENTAL PROCEDURE

Firstly the components and instruments are connected properly with the experimental set up for proper operation; the blower is then switched on after checking all the connections. Every joint has to be checked and made leak proof to eliminate errors. The adjustments of air flow are done through the control valve after making the micrometer and U-tube manometer levelled. Experimental data are collected to calculate the heat transfer coefficient and friction factor. The first reading of the data is to be noticed only after reaching the steady conditions.

Each change in the rate of flow of air the system should attain a steady state before the data were recorded. The system takes approximate 40-45 minutes to attain a Quasi-steady state on every operating condition change. The temperature of the flowing air through the duct was maintained greater than 10^0C to obtain the accurate results since the accuracy of heat transfer coefficient calculation is affected by the temperature measurement. The temperature difference between the heated plate and bulk air temperature has been kept more than 20^0C. When quasi-static condition is reached, current and voltage of the heater assembly by using an ammeter and voltmeter, inlet, outlet and plate temperature by using U-tube manometer and pressure drop across the duct by using micro manometer have been recorded. For the different arc angle of artificial roughness the mass flow rate of air is calculated. The Reynolds number range is varied in between 3000 to 14000.

The parameters measured during the experiments were inlet air temperature, outlet air temperature and plate temperature by using digital multimeter and thermocouple wires, pressure drop across the duct by using micro manometer and pressure drop across the orifice plate by using U-tube manometer. There is only one thermocouple wire for measuring inlet air temperature, whereas five thermocouple wires place at the outlet sections to measure outlet temperature and six thermocouple wires place at the outlet sections to measure plate temperature.

4. ROUGHNESS PARAMETERS

4.1 Parametric Range

Table 4.1: Parametric Range

Parameters	Range/Values
Reynolds Number, Re	3000-14000
Relative Roughness, p/e	8.33
Relative roughness height, e/D_h	0.027
Angle of attack (α)	30^0,45^0,60^0,75^0

Aspect ratio of duct, W/H	8
Hydraulic diameter, D_h (mm)	44.44
Roughness pitch, p (mm)	10
Roughness height, e (mm)	1.2
Insolation, I (W/m^2)	950-970

4.2 Data Reduction

The experimental data, such as air and plate temperatures at various locations in the duct was recorded under quasi-steady state conditions at different mass flow rates (Reynolds number) of air. For mass flow measurement pressure drop across orifice has been measured. This data was used to calculate heat transfer rate of air flowing in the duct. The following equations are used to calculate the Mean air and plate temperature (T_{Fav}, T_{Pavg}), Pressure drop across the orifice, ΔP_o mass flow rate 'm', velocity measurement, V, Reynolds number, Re, Heat transfer rate, Qa, Nusselt number, Nu, Friction factor, f, Thermal efficiency, η^{th}, Heat transfer coefficient and Thermal Hydraulic Performance, THP.

4.2.1 Mean Air and Plate Temperature

The average flow temperature is the arithmetic mean of temperature measured at the inlet and exit of the test section. Thermocouple wires are arranged at equidistance on the entire length of the plate, therefore it is the average reading of six points located at the distance 214 mm on the plate.

$$T_{Fav} = (T_i+T_{Paav})/2 \quad (1)$$

$$T_{Pavg} = (T1+T2+T3+T4+T5+T6)/6 \quad (2)$$

4.2.2 Pressure Drop Calculation

Across the orifice plate, pressure drop is calculated by the following equations:

$$\Delta P_o = \Delta h \times 9.81 \times \rho_m \quad (3)$$

Here ΔP_o = Difference in Pressure, Pa

ρ_m = Density of manometric fluid, kg/m^3

Δh = Difference of mercury level inside U-tube manometer, m

4.2.3 Mass Flow Calculations

Mass flow rate of air has been calculated from pressure drop measurement across the orifice plate by using the following equations:

$$m = C_d \times A_o \times [2\rho\Delta P_o/(1-\beta^4)]^{0.5} \quad (4)$$

Here m = mass flow rate of air, kg/s

C_d = Coefficient of discharge of orifice i.e. 0.62

A_o = Area of orifice plate, $1.288 \times 10^{-3,}$ m^2

ρ_a = Density of air, kg/m^3

β = Dia ratio i.e. 40.5 / 81 = 0.5

4.2.4 Velocity Measurement

$$V = m/ \rho_a WH \quad (5)$$

Here m = mass flow rate, kg/s

ρ_a = Density of air i.e. 1.1415, kg/m^3

H = Height of duct, 0.025, m

W = Width of the duct, 0.2, m

4.2.5 Reynolds Number

For flow of the air inside the duct, Reynolds number is calculated by:

$$R_e = \rho_v D_h/\mu \quad (6)$$

Where μ = Dynamic viscosity, kg-m/s

D_h = Hydraulic dia = 4WH / (W+H), m

4.2.6 Equivalent Diameter

D_h = 4* Area of cross-section/wetted perimeter

D_h = 4* A/P= 4WH/ 2(W+H)

4.2.7 Heat Transfer Rate

The Heat transfer rate is calculated by:

$$Q_a=mc_p(To–T_i), KJ \quad (7)$$

and for the heated test section, heat transfer rate is given by

$$Q_a = hA_p(T_{pav}–T_{fav}), KJ \quad (8)$$

4.2.8 Nusselt Number

The heat transfer coefficient has been used to determine the Nusselt number and is defined as

$$N_u = hD/k \quad (9)$$

Where k is the thermal conductivity of the air at mean plate temperature and D_h is the hydraulic diameter, m

4.2.9 Friction Factor

Friction factor is calculated by:

$$f=(2\Delta P_d D_h/4\rho LV^2) \quad (10)$$

Where $(\Delta P)_d$= Pressure drop in N/m^2 for 1.36 m length

4.3.0 Thermal Efficiency

The thermal efficiency is calculated by

$$\eta_{th} = m \times c_p \times \Delta T / I \times A_P \quad (11)$$

Where I is the heat flux or Insolation, W/m^2

A_P is the absorber plate area, m^2

4.3.1 Convective Heat Transfer Coefficient

$$h = Q_a / A_p (T_{pm} - T_{fm}) \quad (12)$$

Where,

Qa = Heat gained by air, Watt

A_p= Area of absorber plate, m^2

T_{pm}= Mean Temperature of plate, °C

T_{fm}= Mean Temperature of fluid flowing, °C

4.3.2 Thermo-Hydraulic Performance

$$THP = (Nu/Nus)/(f/fs)^{1/3} \quad (13)$$

Where,

Nu_r = Nusselt no. of roughened plate

Nus = Nusselt no. of smooth plate

f & fs are the corresponding value of friction factor

5. VALIDATION OF EXPERIMENTAL DATA

Before collecting the actual data, the validation of test setup was done by conducting experiments for a smooth duct. The friction factor and Nusselt number values from these experimental data were compared with the theoretical values obtained from the Dittus Boelter equation for the nusselt number and modified Blasius equation for the friction factor.

The **Dittus and Boelter Equation** to obtain the Nusselt number for a smooth rectangular duct is given below:

$$\mathbf{Nu = 0.024\ Re^{0.8}\ Pr^{0.4}}$$

The **Modified Blasius Equation** to obtain friction factor for a smooth rectangular duct is given below:

$$\mathbf{f = 0.085\ Re^{-0.25}}$$

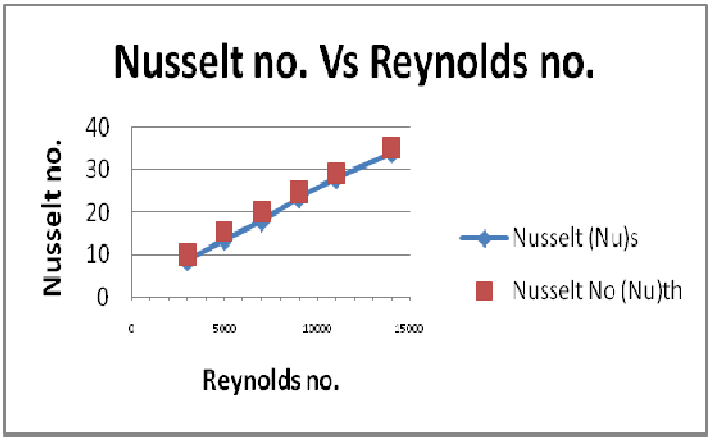

Figure 4: Comparison of Experimental and Formulated Value of Nusselt Number vs Reynolds Number for Smooth Plate

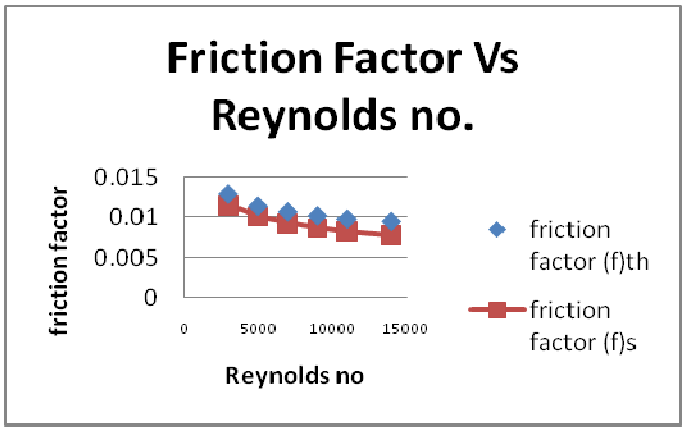

Figure 5: Comparison of Experimental and Formulated Value of Friction Factor vs Reynolds No. for Smooth Plate

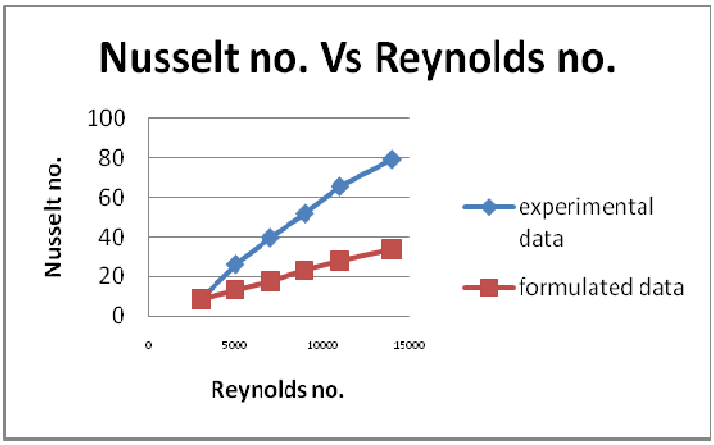

Figure 6: Nusselt No. vs Reynolds No. for Roughness Plate 1

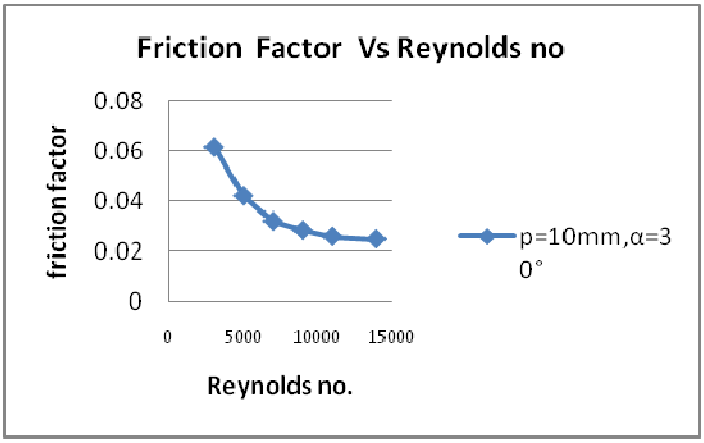

Figure 7: Friction Factor vs Reynolds No. for Roughness Plate 1

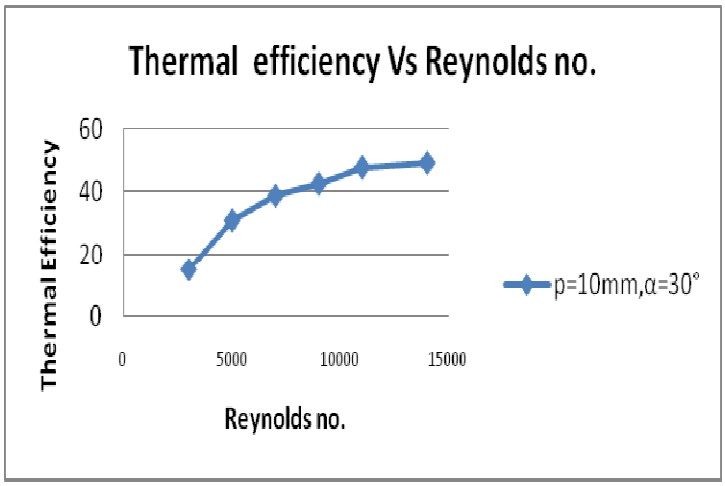

Figure 8: Thermal Efficiency vs Reynolds No. for Roughness Plate 1

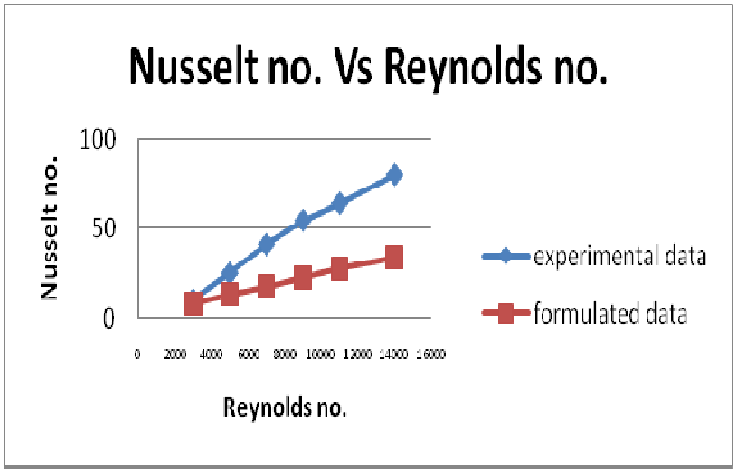

Figure 9: Nusselt Number Vs Reyonlds No. for Roughness Plate 2

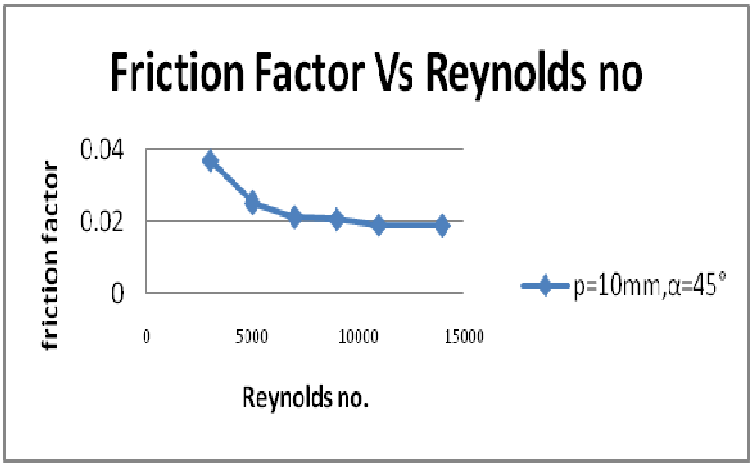

Figure 10: Friction Factor vs Reynolds No. for Roughness Plate 2

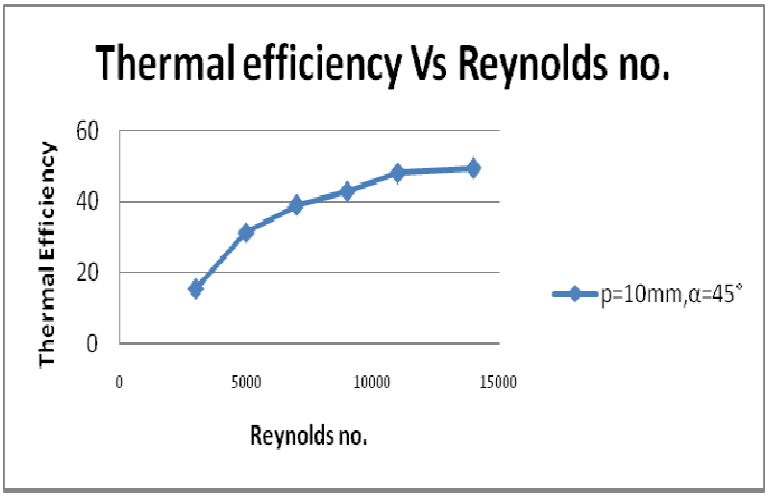

Figure 11: Thermal Efficiency vs Reynolds No. for Roughness Plate 2

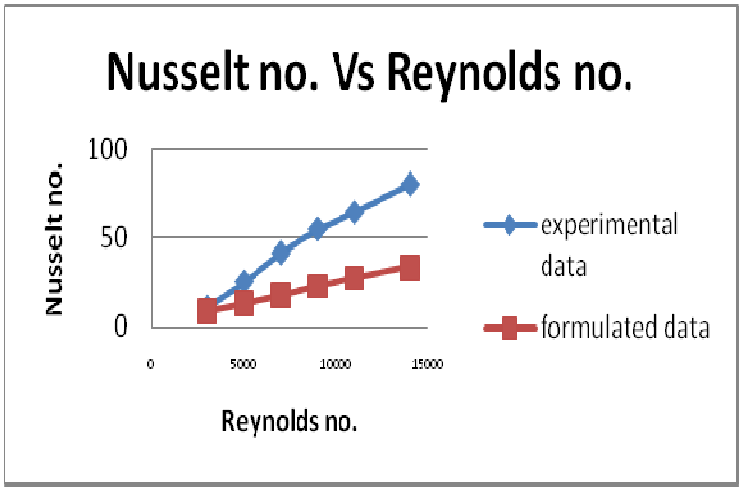

Figure 12: Nusselt Number vs Reyonlds No. for Roughness Plate 3

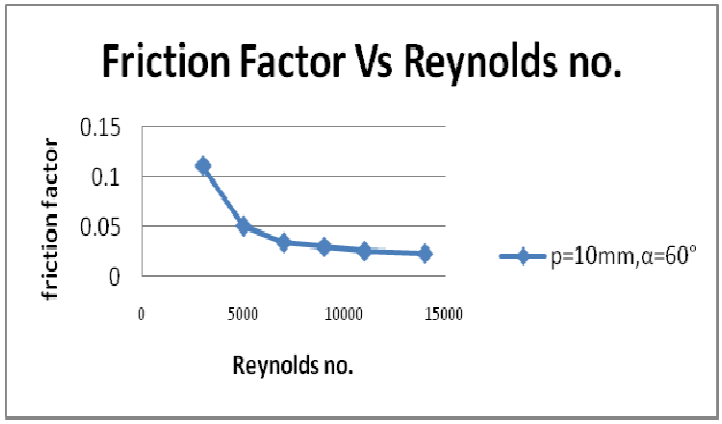

Figure 13: Friction Factor vs Reynolds No. for Roughness Plate 3

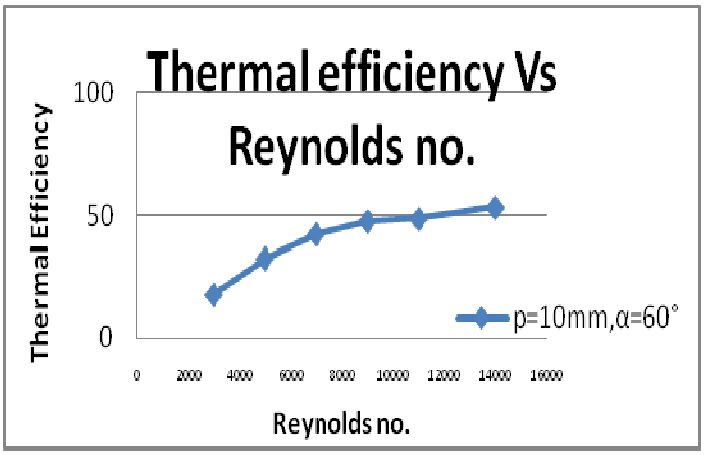

Figure 14: Thermal Efficiency vs Reynolds No. for Roughness Plate 3

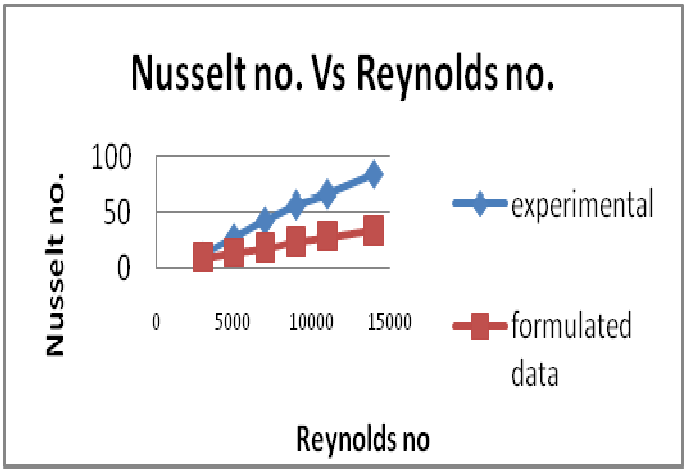

Figure 15: Nusselt no. vs Reynolds No. for Roughness Plate 4

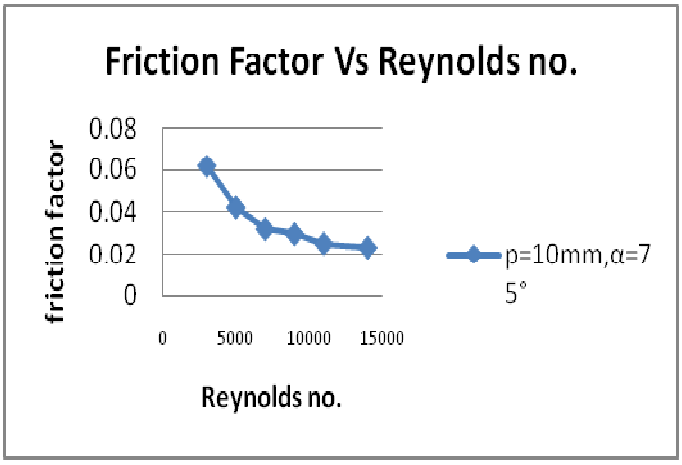

Figure 16: Friction Factor vs Reynolds No. for Roughness Plate 4

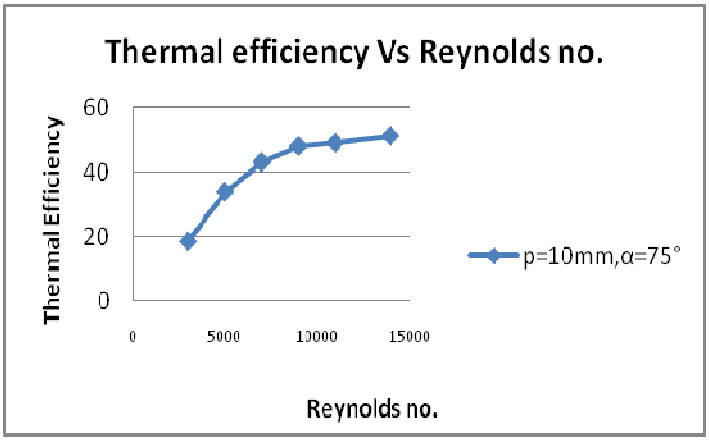

Figure 17: Thermal Efficiency vs Reynolds No. for Roughness Plate 4

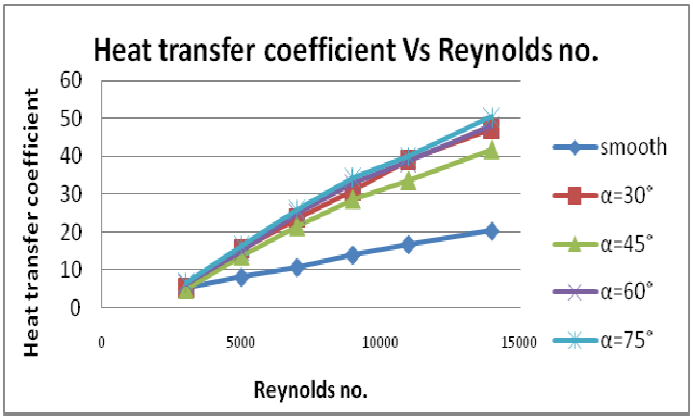

Figure 18: Comparison of Heat Transfer Coefficient vs Reynolds no. for Different Roughness Plates Having Pitch 10mm with Smooth Plate

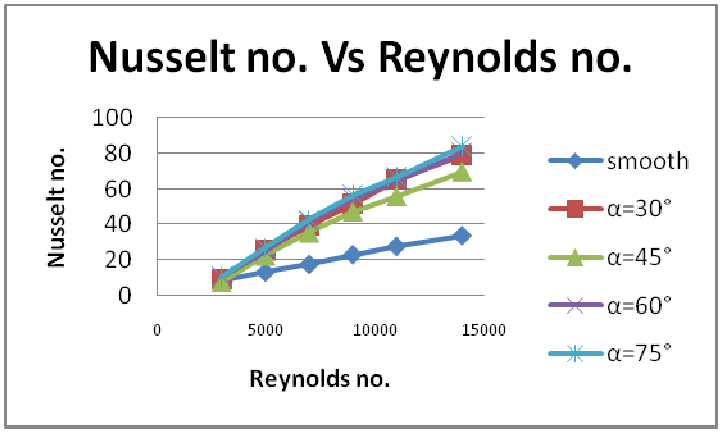

Figure 19: Comparison of Nusselt No. vs Reynolds No. for Different Roughness Plates Having Pitch 10mm with Smooth Plate

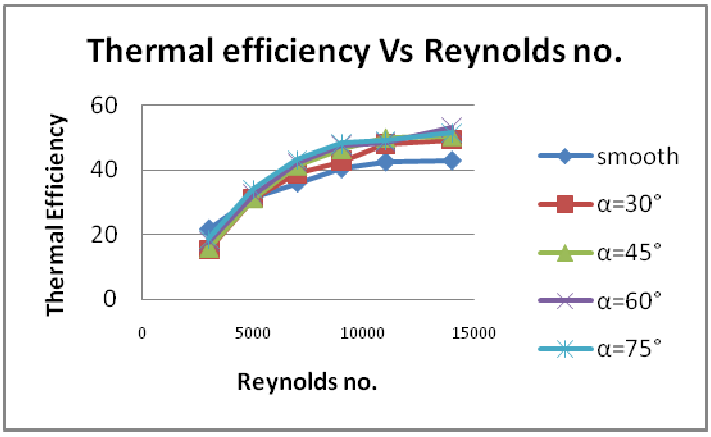

Figure 20: Comparison of Thermal Efficiency vs Reynolds No. for Different Roughness Plates Having Pitch 10mm with Smooth Plate

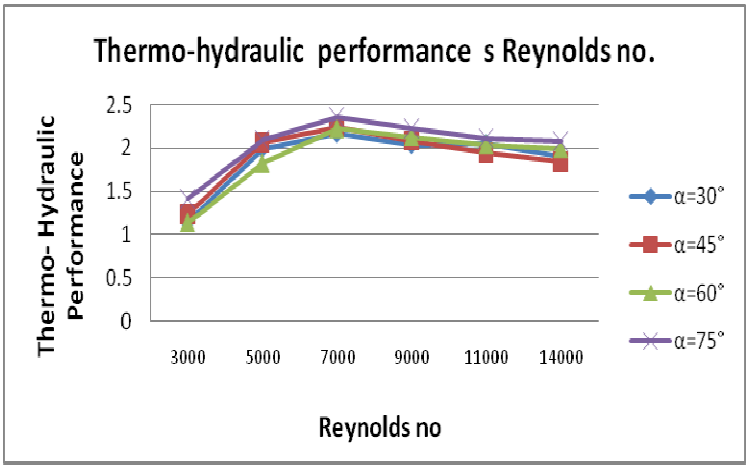

Figure 21: Graph Showing THP Vs Re for Different Roughness Plates Having 10mm Pitch

6. RESULT & DISCUSSIONS

In this research based on experiments, the influence of different roughness parameters and various flow arrangements for the heat transfer for the air flow in the rectangular duct is analysed. The results with respect to the different roughness parameters are compared to the maintenance flow conditions of smooth duct similar to those of the improvement of the heat transfer coefficient, the increase of the Nusselt number and the friction factor.

The experimental data showing the increase in the heat transfer coefficient with the increase in the value of the Reynolds number give us a graph that is shown in Figure 18.

The increase in the value of the Nusselt number with an increase in the Reynolds number. The value of the Nusselt number shows an increase of 1.26 to 2.478 times compared to the Nusselt number of smooth plate. The Reynolds number varies between 3000 and 14000, the highest value of the Nusselt number is 2,478 times observed in the Reynolds number 14000 with a roughness pitch of 10 mm and an arc angle of 75 °.

The thickness of the boundary layer decreases with increasing Reynolds number, which increases convective heat transfer between the absorbent plate and the air by decreasing the convective resistance that produces an increase in the number of Nusselt. The graph between the Nusselt number and the Reynolds number is shown in Figure 19 for the rough and smooth plate.

The increase in thermal efficiency with the increase in the Reynolds number is carried out at a very fast rate initially and then at a decreasing rate. The graph showing the change in thermal efficiency with the increase in the Reynolds number is represented in Figure 20.

Thermo hydraulics is the study of hydraulic flow in thermal systems. As we increase the Reynolds number, the Thermo-Hydraulic Performance (THP) shows an increase up to the value of the Reynolds number 7000, after THP starts to decrease slightly with the increase of the Reynolds number.

This change is observed due to the relative effect of the variation in the heat transfer coefficient and the friction factor. The minimum value of the thermo hydraulic performance is observed in Reynolds number 3000, the pitch of the roughness element 10 mm and the angle of the arc 30^0, while the maximum value of the thermohydraulic efficiency is observed in Reynolds number 7000, the pitch of the roughness element 10 mm and the arc of the angle 30^0, after THP starts to decrease shown in Figure 21.

The thermo hydraulic performance parameter is also known as an efficiency parameter. After all the comparison of the different double arc reverse shape roughness plates with the smooth plate, we find that the thermo hydraulic performance of the double arc reverse shaped roughness geometry is better and can be used for efficient heat transfer.

6. CONCLUSIONS

Following conclusion has been drawn:

- Convective heat transfer coefficient and Nusselt number increases with the increase in Reynolds number for Double arc reverse shape roughness. The increase in Nusselt number is 1.26 to 2.478 times as compared to smooth plate
- Roughness also increases the friction factor value, but increment in its value is small as compared to increase in

heat transfer coefficient. The increase in friction factor is 1.40 to 1.74 times as compared to smooth plate.

- Thermo-hydraulic performance shows variation first increasing and then decreasing with respect to increase in the Reynolds number.
- The maximum enhancement in the Nusselt number is found to be 2.478 for pitch 10 mm, arc, angle 750 with Reynolds number 14000 as compared to smooth plate.
- The maximum increase in friction factor is noticed as 1.74 times for pitch 10 mm, arc, angle 750 with Reynolds number 14000 as compared to smooth plate.
- The maximum improvement in Thermo-hydraulic performance is observed at Reynolds number 7000, the pitch of roughness element 10mm and arc angle 750 in comparison to the smooth plate after that it starts deceasing with an increase in Reynolds number.
- It is observed that there is variation of heat transfer coefficient with the Reynolds number and arc angle both. As the Reynolds number is increased at a constant arc angle, heat transfer coefficient value increases.
- Heat transfer coefficient shows an increase with increase in arc angle at constant Reynolds number, but this increment may or may not be continuous.
- Thermal efficiency also shows the variation with arc angle and Reynolds number. As the Reynolds number increases, continuous increment in thermal efficiency is noticed and similar effect is observed with arc angle but the increment is small.
- The maximum value of Thermal efficiency is observed for the roughness plate having 10 mm pitch, arc, angle 600 having a Reynolds number as 14000.

REFERENCES

1. *Sukhatme SP, Nayak JP. 2011 Solar energy. 3rd ed. NewDelhi: Tata McGrawHill.*
2. *Tyagi, V. V., Panwar, N. L., Rahim, N. A., & Kothari, R. (2012). Review on solar air heating system with and without thermal energy storage system. Renewable and Sustainable Energy Reviews, 16(4), 2289-2303.*
3. *Khan BH. 2012 Non-conventional energy resources. 2nd ed. NewDelhi: Tata McGrawHill.*
4. *Prasad, K., & Mullick, S. C. (1983). Heat transfer characteristics of a solar air heater used for drying purposes. Applied Energy, 13(2), 83-93.*
5. *Prasad, B. N., & Saini, J. S. (1988). Effect of artificial roughness on heat transfer and friction factor in a solar air heater. Solar energy, 41(6), 555-560.*
6. *Han, J. C., Ou, S., Park, J. S., & Lei, C. K. (1989). Augmented heat transfer in rectangular channels of narrow aspect ratios with rib turbulators. International Journal of Heat and Mass Transfer, 32(9), 1619-1630.*
7. *Gupta, D., Solanki, S. C., & Saini, J. S. (1997). Thermohydraulic performance of solar air heaters with roughened absorber plates. Solar Energy, 61(1), 33-42.*
8. *Saini, R. P., & Saini, J. S. (1997). Heat transfer and friction factor correlations for artificially roughened ducts with expanded metal mesh as roughness element. International Journal of Heat and Mass Transfer, 40(4), 973-986.*

9. Karwa R, Solanki SC, Saini JS, Heat transfer coefficient and friction factor correlations for the transitional flow regime in rib-roughened rectangular ducts. International Journal of Heat and Mass Transfer, 42, 1999, 1597–1615.
10. Verma SK, Prasad BN.2000 Investigation for the optimal thermo hydraulic performance of artificially roughened solar air heaters. Renewable Energy. 20: 19–36.
11. Karwa, R., Solanki, S. C., & Saini, J. S. (2001). Thermo-hydraulic performance of solar air heaters having integral chamfered rib roughness on absorber plates. Energy, 26(2), 161-176.
12. Momin, A. M. E., Saini, J. S., & Solanki, S. C. (2002). Heat transfer and friction in solar air heater duct with V-shaped rib roughness on absorber plate. International journal of heat and mass transfer, 45(16), 3383-3396.
13. Bhagoria, J. L., Saini, J. S., & Solanki, S. C. (2002). Heat transfer coefficient and friction factor correlations for rectangular solar air heater duct having transverse wedge shaped rib roughness on the absorber plate. Renewable Energy, 25(3), 341-369.
14. Sahu, M. M., & Bhagoria, J. L. (2005). Augmentation of heat transfer coefficient by using 90 broken transverse ribs on absorber plate of solar air heater. Renewable energy, 30(13), 2057-2073.
15. Karmare, S. V., & Tikekar, A. N. (2007). Heat transfer and friction factor correlation for artificially roughened duct with metal grit ribs. International Journal of Heat and Mass Transfer, 50(21-22), 4342-4351.
16. Aharwal, K. R., Gandhi, B. K., & Saini, J. S. (2008). Experimental investigation on heat-transfer enhancement due to a gap in an inclined continuous rib arrangement in a rectangular duct of solar air heater. Renewable energy, 33(4), 585-596.
17. Kumar, A., Bhagoria, J. L., & Sarviya, R. M. (2009). Heat transfer and friction correlations for artificially roughened solar air heater duct with discrete W-shaped ribs. Energy Conversion and Management, 50(8), 2106-2117.
18. Hans VS, Saini RP, Saini JS, 2010 Heat transfer and friction factor correlations for a solar air heater duct roughened artificially with multipleV-ribs. Solar Energy, 84, 898–911.
19. Sethi, M., & Thakur, N. S. (2012). Correlations for solar air heater duct with dimpled shape roughness elements on absorber plate. Solar Energy, 86(9), 2852-2861.
20. Yadav, S., & Kaushal, M. (2013). Nusselt number and friction factor correlations for solar air heater duct having protrusions as roughness elements on absorber plate. Experimental Thermal and Fluid Science, 44, 34-41.
21. Kishor, K. Fe Thermal Analysis and Experimental Validation on the Components of Si Engines.
22. Singh, A. P. (2014). Heat transfer and friction factor correlations for multiple arc shape roughness elements on the absorber plate used in solar air heaters. Experimental Thermal and Fluid Science, 54, 117-126.
23. Lanjewar, A. M., Bhagoria, J. L., & Agrawal, M. K. (2015). Review of development of artificial roughness in solar air heater and performance evaluation of different orientations for double arc rib roughness. Renewable and Sustainable Energy Reviews, 43, 1214-1223.
24. Maithani, R., & Saini, J. S. (2016). Heat transfer and friction factor correlations for a solar air heater duct roughened artificially with V-ribs with symmetrical gaps. Experimental Thermal and Fluid Science, 70, 220-227.
25. Hans and Gills J S. 2017 “Heat transfer and friction factor correlation for a solar air heater duct roughened artificially with broken arc rib” Experimental Thermal and fluid Science 80, 77-89.
26. Gabhane, M. G., & Kanase-Patil, A. B. (2017). Experimental analysis of double flow solar air heater with multiple C shape roughness. Solar Energy, 155, 1411-1416.